

Cite this: *Digital Discovery*, 2024, 3, 163

# ExpFlow: a graphical user interface for automated reproducible electrochemistry†

Rebekah Duke,<sup>a</sup> Siamak Mahmoudi,<sup>a</sup> Aman Preet Kaur,<sup>a</sup> Vinayak Bhat,<sup>a</sup> Ian C. Dingle,<sup>b</sup> Nathan C. Stumme,<sup>c</sup> Scott K. Shaw,<sup>c</sup> David Eaton,<sup>b</sup> Asmund Vego<sup>b</sup> and Chad Risko<sup>\*ab</sup>

Reproducible data and results underpin the credibility and integrity of research findings across the sciences. However, experiments and measurements conducted across laboratories, or by different researchers, are often hindered by incomplete or inaccessible procedural data. Additionally, the time and resources needed to manually perform repeat experiments and analyses limit the scale at which experiments can be reproduced. Both improved methods for recording and sharing experimental procedures in machine-readable formats and efforts towards automation can be beneficial to circumvent these issues. Here we report the development of ExpFlow, a data collection, sharing, and reporting software currently customized for electrochemical experiments. The ExpFlow software allows researchers to systematically encode laboratory procedures through a graphical user interface that operates like a fill-in-the-blank laboratory notebook. Built-in calculators automatically derive properties such as diffusion coefficient and charge-transfer rate constant from uploaded data. Further, we deploy ExpFlow procedures with robotic hardware and software to perform cyclic voltammetry (CV) experiments in triplicate for eight well-known electroactive systems. The resulting oxidation potentials and diffusion coefficients are consistent with literature-reported values, validating our approach and demonstrating the utility of robotic experimentation in promoting reproducibility. Ultimately, these tools enable automated and (semi) autonomous cyclic voltammetry experiments and measurements that will facilitate high-throughput experimentation, reproducibility, and eventually data-driven electrochemical discovery.

Received 17th August 2023  
Accepted 4th December 2023

DOI: 10.1039/d3dd00156c

rsc.li/digitaldiscovery

## Introduction

Chemistry has seen a growing emphasis on reproducibility, driven by the recognition that the credibility and integrity of scientific findings heavily rely on the ability to reproduce experimental results.<sup>1–5</sup> However, reproducing published results is not always straightforward. Procedures described in scientific literature are often incomplete or ambiguous and may unintentionally lack critical details. This lack of comprehensive and standardized documentation hampers the ability of other scientists to reproduce experiments and measurements. Additionally, experimental data can be tedious and time consuming to produce, disincentivizing scientists from reproducing published results and thus hampering robust scientific conclusions.

Automation has emerged as a pivotal component in both enhancing reproducibility and enabling the generation of vast quantities of data.<sup>6–12</sup> Automation increases the quantity of experiments and measurements that can be performed, and can enable greater experimental precision, accuracy, and consistency, much like robotics systems used in assembly-line-based manufacturing. Furthermore, the automated generation of large quantities of experimental data will allow for more big data analysis; rapid advances in the availability and scale of big data in chemistry have generated exciting results already.<sup>13–17</sup> Interfacing automated data collection with big data approaches such as machine learning (ML) and trend analysis can be even more promising.<sup>18–23</sup>

Achieving scientific reproducibility and advancing automation will require the convergence of data, software, domain knowledge, and the development of effective data management frameworks.<sup>19,24</sup> Specifically, it is essential to develop improved methods for recording and sharing experimental procedures, permitting researchers to reproduce and validate results more effectively. Moreover, these captured experimental procedures should be machine-readable, allowing for the translation of human ideas into machine actions. Many research efforts to capture experiment procedural data,<sup>25–29</sup> automate experiments

<sup>a</sup>Department of Chemistry, University of Kentucky, Lexington, Kentucky 40506, USA.  
E-mail: chad.risko@uky.edu

<sup>b</sup>Center for Applied Energy Research, University of Kentucky, Lexington, Kentucky 40511, USA

<sup>c</sup>Department of Chemistry, University of Iowa, Iowa City, Iowa 52242, USA

† Electronic supplementary information (ESI) available. See DOI: <https://doi.org/10.1039/d3dd00156c>



and measurements,<sup>6–8,18,30,31</sup> and incorporate ML into automation<sup>32–34</sup> exist. However, only a few recent efforts exist to systematically capture electrochemistry procedural data and/or automate electrochemistry experiments.<sup>22,35–37</sup> Yet electrochemistry, and especially cyclic voltammetry (CV), holds a crucial role in chemical research, as fields as diverse as drug discovery,<sup>38,39</sup> energy and materials,<sup>40–42</sup> process engineering,<sup>43,44</sup> and environmental chemistry<sup>45</sup> use CV for characterization and analysis. Thus, software to capture electrochemical procedural data and subsequent software and hardware to translate these data into automated CV experimentation and measurements can have broad impact.

Here, we present ExpFlow, a data collection, sharing, and reporting software where electrochemists can systematically encode their laboratory workflows through a graphical user interface. ExpFlow's graphical user interface allows for the creation of standardized, machine-readable procedures that permit both humans and robots to better reproduce datasets. We then demonstrate the use of ExpFlow in executing CV experiments with an automated robotic arm, followed by data processing and results that match well with literature-reported results.

## Methods

### ExpFlow and robotic software

The software ecosystem consists of an experiment data management software with a Python-based web-interface (ExpFlow) and an interface between ExpFlow and the automation hardware with a desktop application. ExpFlow uses the Django<sup>46</sup> web-framework with a MongoDB<sup>47</sup> database to store the experimental information and is hosted on an Apache<sup>48</sup> web server. The interface to the automation hardware uses the Kinova API<sup>49</sup> and Fireworks<sup>50</sup> Python packages and is wrapped into a desktop app with Tkinter.<sup>51</sup>

### System hardware

The robot-enabled CV hardware consists of a Kinova<sup>52</sup> Gen 3 robotic arm with six degrees of freedom. A grid vial stand and vial elevator were designed, 3D-printed, and assembled in-house. A BioLogic SP-50e potentiostat is integrated into the system for cyclic voltammetry measurements. More information on the hardware can be found in ESI Section 2.†

### CV experiments

The electrolyte used for CV experiments was comprised of 0.25 M tetraethylammonium tetrafluoroborate (TEABF<sub>4</sub>) in acetonitrile (ACN). Ferrocene (Fc), *N*-[2-(2-methoxyethoxy)ethyl]-phenothiazine (MEEPT), dimethylphenazine (DMPZ), 4-methoxy-2,2,6,6-tetramethyl-1-piperidinyloxy (4-MeOTEMPO), 1,4-di-*tert*-butyl-2,5-dimethoxybenzene (DBB), 1,4-di-*tert*-butyl-2,5-bis (2-methoxyethoxy)benzene (DBBB), thianthrene (TH) and *N*-ethylcarbazole (ECZ) (Fig. S7†) were individually dissolved at 10 mM in 0.25 M TEABF<sub>4</sub>/ACN (10 mL) in screw capped scintillation glass vials. All solutions were freshly prepared for each trial.

CV experiments were performed on the electro-active solutions using a three-electrode system under ambient conditions. The cell was comprised of a screen-printed electrode fabricated on a ceramic substrate (Pine Research<sup>53</sup>) and an Ag pseudo-reference electrode (Pine Research<sup>53</sup>). The screen-printed electrode contains a 2 mm diameter Au working electrode and a large surface area U-shaped Au counter electrode. The reference electrode was freshly prepared by immersing silver wire in a fritted tube (Pine Research<sup>53</sup>) containing 10 mM silver tetrafluoroborate (AgBF<sub>4</sub>) dissolved in 0.25 M TEABF<sub>4</sub>/ACN. The electrodes were held in place using a grip mount (Pine Research<sup>53</sup>) and a cell cap (Pine Research,<sup>53</sup> fits scintillation vial and grip mount), and connected to the potentiostat using a universal specialty cell connection kit (Pine Research<sup>53</sup>). The electrodes were used as received. A new screen-printed electrode and glass frit for reference electrode was used for each of the eight, three-repeat, experimental trials. CV measurements were performed and data were collected using the BioLogic SP-50e potentiostat. The voltammograms were recorded at scan rates of 25, 50, 75, 100, 200, 300, 400 and 500 mV s<sup>-1</sup>. No solution resistance compensation (*iR* correction) was applied.

## Results and discussion

### ExpFlow: encoding experimental procedures

To tackle the challenges of collecting and analyzing experimental electrochemical data, we created ExpFlow, a data sharing and reporting software targeting electrochemistry that enhances data reusability and facilitates analysis. The procedural and experimental data are divided into three categories for organization and reuse: *Template*, *Experiment*, and *Run* (Fig. 1). The customizable *Template* allows researchers to document experimental steps, *Experiment* specifies experiment

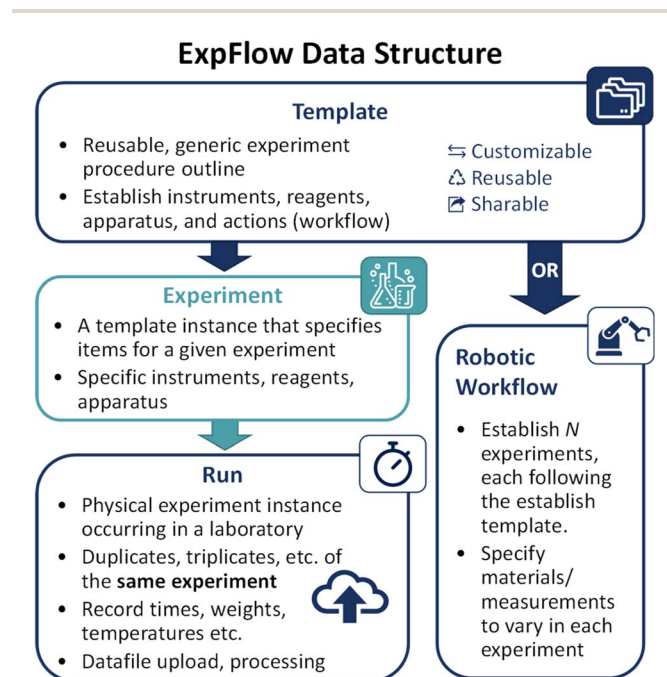


Fig. 1 Schematic showing ExpFlow data organizational structure.



reagents and apparatus, and *Run* works like a fill-in-the-blank lab notebook, where chemists record measurements and attach data files. Built-in calculators perform calculations (e.g., peak splitting, peak potentials, reversibility, diffusion coefficient, charge transfer rate, etc.) (Table S1†). Additionally, an existing *Template* can be cloned, modified, and shared (either among ExpFlow users or *via* download). Each of these pieces are hosted on a web user interface.<sup>54</sup> Procedural and experimental data stored in ExpFlow are comprehensive and machine-readable (specifically *via* the JSON<sup>55</sup> format) so as to enhance reproducibility and enable translation of experiment procedures to robotic experiments.

An ExpFlow *Template* converts experimental procedures into graphs that contain data provenances. The *Template* has categories for *reagent* (e.g., redox material, solvent), *apparatus* (e.g., beaker, electrode) and *instrument* (e.g., potentiostat, spectrometer). In a *Template* graph, nodes (the reagent, apparatus, and instrument categories) are connected by edges that correspond to *actions* (e.g., dispense, heat). Each action contains a start position, an end position, and action parameters (e.g., volume for dispensing liquid, temperature for heating, etc.). As the actions are sequenced, ExpFlow graphs capture the action provenances.

For example, a CV experiment to determine the diffusion coefficient might include redox-active molecule and solvent reagents, a beaker/vial apparatus, and a potentiostat (Fig. 2). Workflow actions might include transferring the liquid solvent and solid solute to the beaker, heating and stirring the solution, measuring the working electrode surface area, and collecting

CV data. In this example, the user might add five collect-CV-data actions because the experiment includes five CV scans, each performed at a different scan rate. Although the *Template* can take time and effort to produce, it can be reused for all related and subsequent experiments.

A single *Template* can be used for multiple *Experiments* where materials (reagents, instruments, etc.) are specified. For instance, the aforementioned *Template* can parent three *Experiments*, each using a different solvent (e.g., water, acetonitrile, and propylene carbonate). When collecting data, a user runs a given experiment any number of times. During an experiment *Run*, the researcher is prompted to fill in embedded run parameters for each action. For example, the liquid-transfer action type prompts the researcher to record the liquid volume, while the heat-and-stir action type prompts the researcher to record the temperature and the stirring time. Data collection action types prompt the researcher to upload a raw data file, in this case, the potentiostat output file. For more information about the ExpFlow data structure, see ESI Section 1.†

A *Template* can also be adapted to a *Robotic Workflow*. After selecting a *Template*, the researcher indicates default measurements for all preparation steps and specifies parameters for all data collection steps. Then, the researcher selects one or more parameters to vary. These variable parameters become the columns of a table with  $n$  rows, where the researcher specifies the variable parameter values for each of  $n$  experiments (Fig. S7†). ExpFlow then produces a machine-readable workflow for  $n$  identically structured experiments where one or more measurement

## Simplified CV Experiment

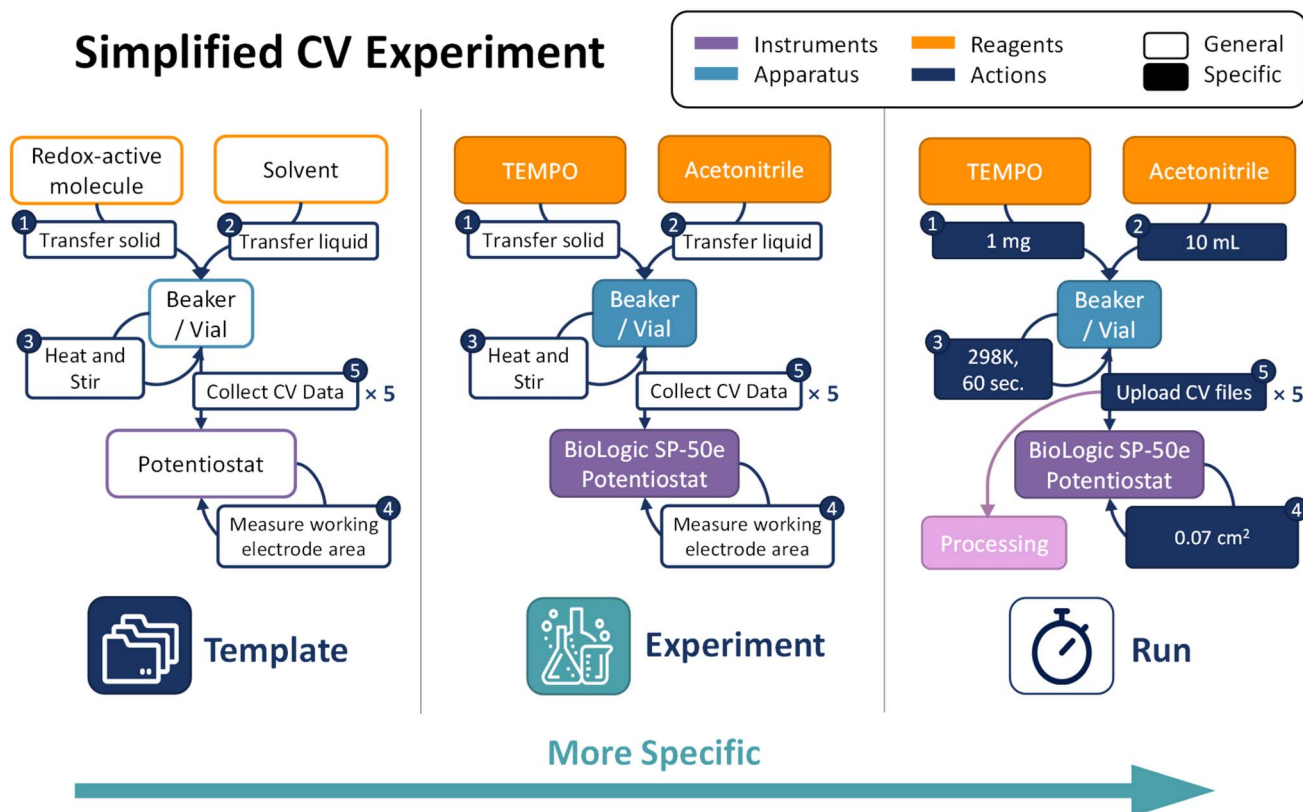


Fig. 2 Schematic demonstrating a simplified CV experiment graph as an ExpFlow *Template*, *Experiment*, and *Run*.



parameters varies for each experiment. These machine-readable workflows can be downloaded for use in robotic experimentation (more details in the next section).

After an experiment is run in ExpFlow, data parsers from the D<sup>3</sup>TaLES API<sup>56</sup> extract data from the uploaded experiment files (Table S1†). Additionally, key metadata are extracted from the *Run* parameter data. For example, the solution temperature is extracted from the heat-and-stir action, and the solution concentration is calculated from the solid-transfer and liquid-transfer actions. All extracted data are displayed on the web user interface where the researcher can inspect and approve the *Run* data. This user interface also contains the ExpFlow calculators (e.g., diffusion coefficient and charge transfer rate constant) for *Runs* with relevant data.

### Proof of concept: automated cyclic voltammetry

ExpFlow provides a platform for researchers to encode the procedure for their electrochemical experiments and measurements. Here, we demonstrate the utility of these machine-readable procedures by translating them into automated CV measurements. First, we assembled the robotic hardware infrastructure needed to run a CV measurement from a pre-mixed solution (Fig. 3). More details about all hardware are provided in ESI Section 2.† We also built the software infrastructure necessary to connect the researcher-created ExpFlow experiment procedures to robotic actions and then communicate collected data back to the researcher (Fig. S5†). Once a researcher creates an ExpFlow *Template* and converts it into a *Robotic Workflow*, the researcher downloads the *Robotic Workflow* to the local robotics computer. Here, through a desktop application, the researcher loads the workflow and assigns reagent locations in the robot space. This step requires human actions as a safety measure to ensure that robotic experiments have human supervision. Finally, a robotics API translates the loaded workflow into robotic actions. Through the local robotics app, the researcher may launch robotic actions to perform the electrochemistry experiment and complete subsequent data processing.

To test and validate the system, we performed CV experiments for eight electro-active systems<sup>57–64</sup> (Fig. S8†): ferrocene (Fc), *N*-[2-(2-methoxyethoxy)ethyl]-phenothiazine (MEEPT), dimethylphenazine (DMPZ), 4-methoxy-2,2,6,6-tetramethyl-1-piperidinyloxy (4-MeOTEMPO), 1,4-di-*tert*-butyl-2,5-dimethoxybenzene (DBB), 1,4-di-*tert*-butyl-2,5-bis(2-methoxyethoxy)benzene (DBBB), thianthrene (TH), and *N*-ethylcarbazole (ECZ). First, we constructed an ExpFlow *Template* for the following process: run one CV scan on a supporting electrolyte solution to confirm electrode cleanliness, select a redox-active solution, perform one benchmark CV scan at 100 mV s<sup>-1</sup> and determine the optimum voltage range, collect eight cyclic voltammograms (each at a different scan rate with the optimum voltage range), and process all data. From this *Template*, we generated a *Robotic Workflow* for performing this experiment on the eight distinct solutions (Fig. S6 and S7†). While this proof-of-concept experiment *Template* utilized the robotic arm only to transfer the solution vials to and from the potentiostat system, it successfully tests the ExpFlow *Template* building interface, the robotic software and hardware, and the automated ExpFlow data processing (see Methods section for more information on solution preparation and experiment procedure). Robotic experiments were then performed from this workflow, and the workflow was completed three times (three trials) with new solutions and electrodes each trial, so the experiment was run in triplicate for each electro-active system. Starting with pre-mixed solutions, one trial of CV experiments and automatic data processing for all eight systems (80 CV's total) took approximately 90 minutes. While the time per measurement is comparable to the time required to perform the measurements manually, the automated data processing (nearly instantaneous) is significantly faster than manually exporting, analyzing, and plotting the data. Moreover, both the measurements and calculations need minimal human oversight.

The scan-rate dependent voltammograms for all eight systems are provided in Fig. 4 and S9.† All compounds except

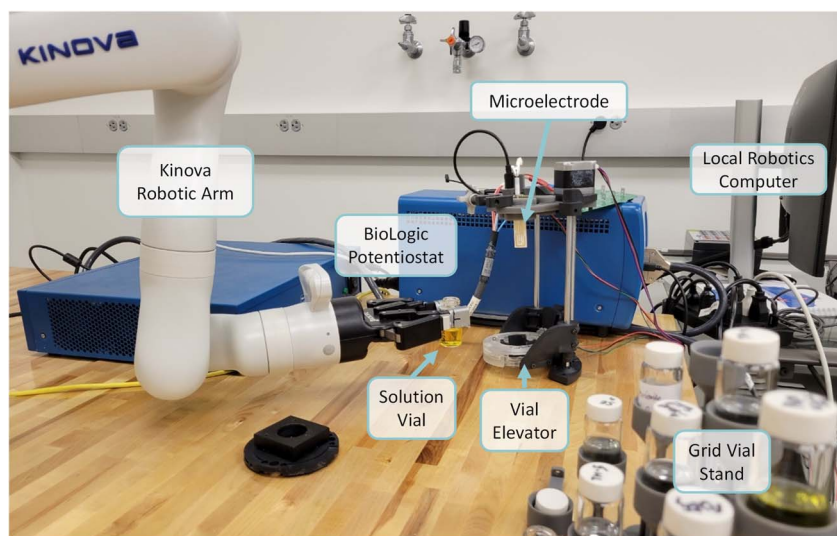


Fig. 3 Image of robotic setup.



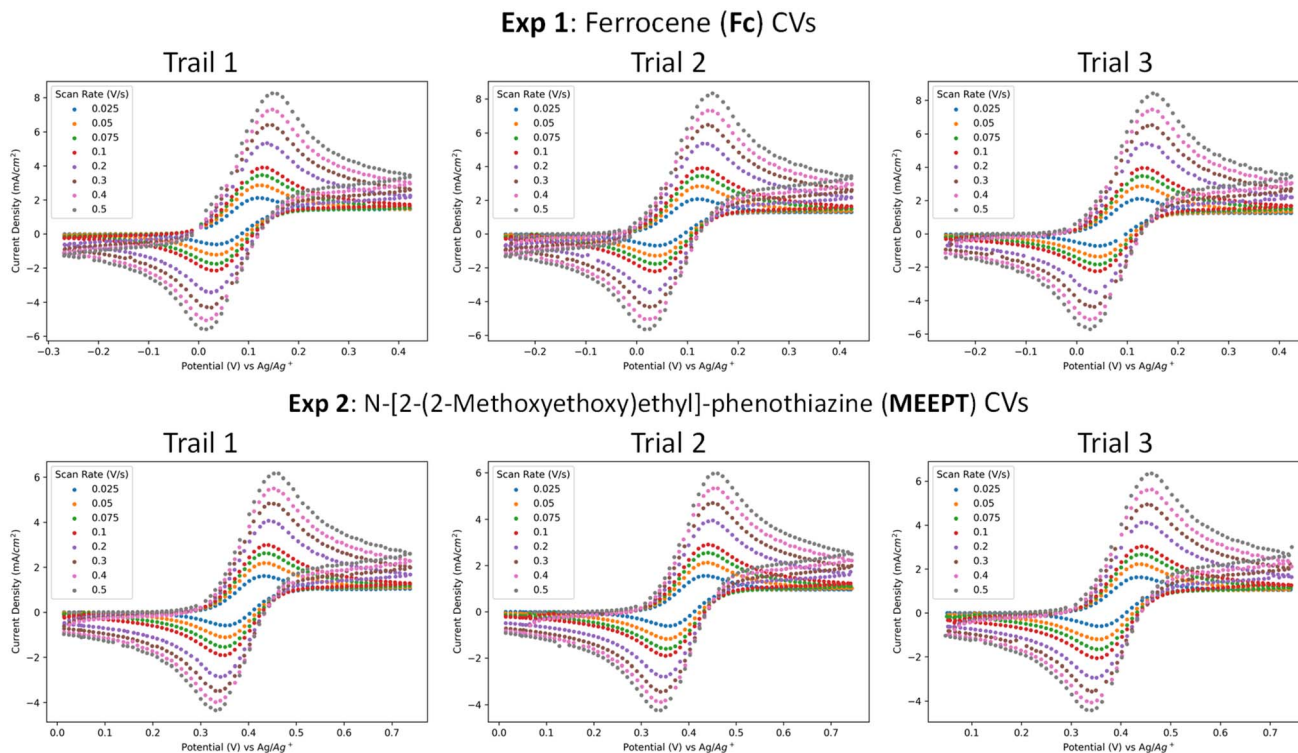


Fig. 4 CV plots produced by the embedded data processors for all trials of Fc (top) and MEEPT (bottom) at 0.01 M in 0.25 M TEABF<sub>4</sub>/acetonitrile electrolyte at room temperature and are reported using IUPAC convention. More information about experimental conditions and all other CVs (Fig. S12†) are located in methods and ESI Section 3.†

ECZ exhibit reversible first oxidation in 0.25 M TEABF<sub>4</sub>/ACN electrolyte and the peak potentials are invariant with the scan rate. DMPZ showed reversible first and second oxidation potentials. Notably, the data processors correctly identified both the first and second oxidations for DMPZ and flagged ECZ, which has a known irreversible first oxidation,<sup>62,65</sup> as irreversible (Fig. S9†). The average peak to peak separation for reversible oxidations at different scan rates is 0.104 V, which is wider than the ideal peak separation for a reversible process. A major factor contributing to wider peaks is the lack of *iR* compensation in our experiments.

For each system, the embedded data processing determined (among other properties) the oxidation potential(s) and cathodic diffusion coefficient, and these were compared with literature-reported values. For example, the measured half-wave redox potential (at 100 mV s<sup>-1</sup>) for Fc of 0.082 ± 0.001 V vs. Ag/Ag<sup>+</sup> aligns well with the literature-reported<sup>66</sup> potential of 0.086 V vs. Ag/Ag<sup>+</sup>. Additionally, the measured diffusion coefficient of 1.73 ± 0.06 × 10<sup>-5</sup> cm<sup>2</sup> s<sup>-1</sup> is consistent with the literature-reported<sup>67</sup> coefficient of 2.10 × 10<sup>-5</sup> cm<sup>2</sup> s<sup>-1</sup>. Similar results were observed for MEEPT, another well studied redox-active system known for its high stability and solubility.<sup>68-70</sup> The measured half-wave redox potential for MEEPT is 0.396 V vs. Ag/Ag<sup>+</sup>, which is comparable with the potential (0.41 V vs. Ag/Ag<sup>+</sup>)<sup>71</sup> reported for *N*-methylphenothiazine. Since there are no literature-reported oxidation potentials for MEEPT vs. Ag/Ag<sup>+</sup>, the potential is estimated relative to Fc/Fc<sup>+</sup> using the potential gathered for Fc in the robotic experiments as the standard. The measured oxidation

potential of 0.314 V vs. Fc/Fc<sup>+</sup> aligns very well with the literature-reported<sup>69</sup> potential of 0.310 V vs. Fc/Fc<sup>+</sup>. The measured diffusion coefficient of 0.93 ± 0.06 × 10<sup>-5</sup> cm<sup>2</sup> s<sup>-1</sup> is also close to the literature-reported<sup>69</sup> coefficient of 1.16 × 10<sup>-5</sup> cm<sup>2</sup> s<sup>-1</sup>.

The collected electrochemical data for all eight systems, compares well with literature-reported results (Fig. 5, see Tables S2 and S3† for raw data).<sup>59,66,67,69,71-77</sup> The robotic experiment oxidation values have an almost perfect one-to-one correlation with literature-reported values. The robotic experiment diffusion coefficients are consistent with the range of values observed for redox-active molecules in ACN-based electrolytes<sup>59,67,69,72,78</sup> and correlate well with the literature-reported values. We hypothesize that the slight differences observed here when compared with literature-reported values are primarily due to the differences in conditions used for estimating these values. For example the diffusion coefficient of 1.73 × 10<sup>-5</sup> cm<sup>2</sup> s<sup>-1</sup> observed for Fc at 10 mM in 0.25 M TEABF<sub>4</sub>/ACN at 22 °C in our experiment is compared to literature-reported value of 2.10 × 10<sup>-5</sup> cm<sup>2</sup> s<sup>-1</sup> obtained for Fc at 10 mM in 0.1 M TEABF<sub>4</sub>/ACN at 25 °C. Similarly, for MEEPT (10 mM in 0.25 M TEABF<sub>4</sub>/ACN; experimentally observed 0.93 × 10<sup>-5</sup> cm<sup>2</sup> s<sup>-1</sup>) it is compared to conditions (1 mM in 0.1 M TEABF<sub>4</sub>/ACN; literature-reported 1.16 × 10<sup>-5</sup> cm<sup>2</sup> s<sup>-1</sup>) where both the redox-active molecule and salt concentrations are different. Electrolyte composition and temperature play an important role for these calculations.<sup>56</sup> Accounting for these variations, our results validate our robotic setup and data processing, and demonstrate the potential for machine-readable



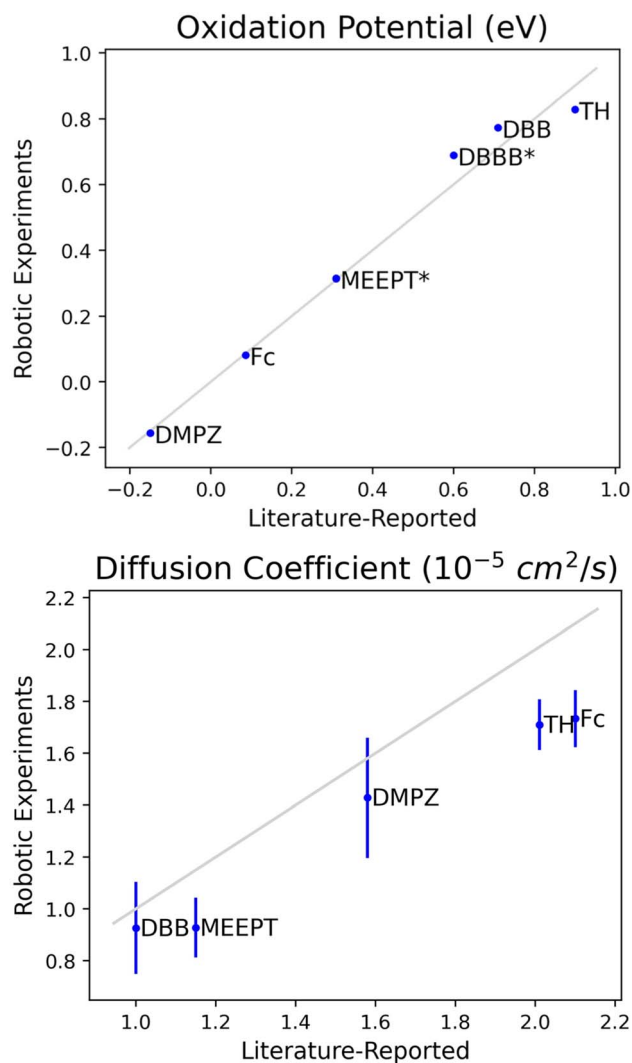


Fig. 5 Comparison of values produced during robotic experimentation and literature-reported values for oxidation potential (top) and diffusion coefficient (bottom). Robotic experimental values are reported as the average value across the three trials where the error bars are twice the standard deviation. The gray line represents an ideal one-to-one correlation between the robotic and literature-reported values. All robotic potentials are measured vs. Ag/Ag<sup>+</sup>. For all raw data, see Tables S2 and S3.† For comparison, literature-reported oxidation potentials are reported referenced to Ag/Ag<sup>+</sup>, except for MEEPT and DBBB (as denoted by the \*); the oxidation potentials for MEEPT and DBBB are estimated relative to Fc/Fc<sup>+</sup> using the potential measured for Fc in the robotic experiments as the standard.

procedures and automation to facilitate high-throughput experiments.

## Conclusions

Here we present ExpFlow, a software that allows systematic encoding of laboratory workflows through a graphical user interface. These encoded workflows standardize experimental practices to capture all experiment metadata with the aim of enhancing reproducibility. Currently, ExpFlow supports data parsing for CV experiments. Machine-readable ExpFlow

procedures also facilitate the translation of human-developed laboratory procedures to robotic experimentation, as we demonstrate for robotic electrochemistry experiments. We used an ExpFlow *Template* and a robotic hardware and software setup to perform automated electrochemistry experiments in triplicate for eight well-known electroactive systems. The resulting oxidation potentials and diffusion coefficients are consistent with literature-reported values, validating the setup and demonstrating the utility of robotic experimentation in promoting reproducibility.

While this proof-of-concept robotics phase demonstrates the software and basic hardware needed for translating human-conceived electrochemistry experiments to robotic actions, there is still room for improvement. Future additions may include liquid dispensing and solution mixing as well as additional characterization metrics such as viscosity, solubility, and spectroscopic characterization. We also plan to fine-tune the potentiostat data collection methods (*e.g.*, incorporate *iR* compensation and argon flushing) to ensure that the robotic experiments produce high quality data on par with current literature standards.<sup>41,79</sup> Ultimately, the advances demonstrated here will facilitate reproducibility, automated labs, and eventually autonomous design of experiments<sup>80</sup> for electrochemistry.

## Data availability

The ExpFlow software and interface can be found at <https://d3tales.as.uky.edu/expflow/>. Documentation can be found at <https://d3tales.as.uky.edu/expflow/docs>. Further details on ExpFlow operation, the robotic data flow, hardware descriptions, the ExpFlow template used to run the robotic experiments, properties determined as a function of cyclic voltammetry (CV) processing, and all materials and data from the CV experiments can be found in the ESI.†

## Author contributions

R. D.: data curation, formal analysis, investigation, methodology, software, visualization, writing – original draft, writing – review & editing. S. M.: methodology, software, writing – review & editing. A. K.: data curation, investigation, methodology, validation, writing – review & editing. I. C. D.: software, resources. N. C. S.: data curation, validation. S. K. S.: supervision, funding acquisition, writing – review & editing. V. B.: conceptualization, software, writing – review & editing. A. V.: conceptualization, supervision, writing – review & editing. D. E.: conceptualization, supervision, funding acquisition, writing – review & editing. C. R.: conceptualization, project administration, supervision, funding acquisition, writing – review & editing.

## Conflicts of interest

There are no conflicts to declare.

## Acknowledgements

This work was generously supported by the National Science Foundation (NSF) under Cooperative Agreement Number



2019574. We thank Dr Andrew Horvath for testing ExpFlow and providing perspective on the software design, and we thank Dr Judy Jenkins for her expert advice regarding the robotic electrochemistry setup. Finally, we wholeheartedly thank the entire D<sup>3</sup>TaLES (<https://d3tales.as.uky.edu/>) team for their insights into the development of this software and robotic system.

## References

- 1 D. A. Leins, S. B. Haase, M. Eslami, J. Schrier and J. T. Freeman, Collaborative methods to enhance reproducibility and accelerate discovery, *Digital Discovery*, 2022, 2, 12–27, DOI: [10.1039/d2dd00061j](https://doi.org/10.1039/d2dd00061j).
- 2 M. Baker, 1,500 scientists lift the lid on reproducibility, *Nature*, 2016, 533(7604), 452–454, DOI: [10.1038/533452a](https://doi.org/10.1038/533452a).
- 3 M. Abolhasani and E. Kumacheva, The rise of self-driving labs in chemical and materials sciences, *Nature Synthesis*, 2023, 2(6), 483–492, DOI: [10.1038/s44160-022-00231-0](https://doi.org/10.1038/s44160-022-00231-0).
- 4 R. G. Bergman and R. L. Danheiser, Reproducibility in Chemical Research, *Angew. Chem., Int. Ed.*, 2016, 55(41), 12548–12549, DOI: [10.1002/anie.201606591](https://doi.org/10.1002/anie.201606591).
- 5 National Academies of Sciences E., and Medicine, Policy and Global Affairs, Committee on Science, Engineering Medicine, and Public Policy, Board on Research Data and Information, Division on Engineering and Physical Sciences, Committee on Applied and Theoretical Statistics, Board on Mathematical Sciences and Analytics, Division on Earth and Life Studies, Nuclear and Radiation Studies Board, Division of Behavioral and Social Sciences and Education, Committee on National Statistics, Board on Behavioral, Cognitive, and Sensory Sciences and Committee on Reproducibility and Replicability in Science, *Reproducibility and Replicability in Science*, National Academies Press (US), Washington (DC), 2019, DOI: [10.17226/25303](https://doi.org/10.17226/25303).
- 6 P. A. Beaucage and T. B. Martin, The Autonomous Formulation Laboratory: An Open Liquid Handling Platform for Formulation Discovery Using X-ray and Neutron Scattering, *Chem. Mater.*, 2023, 35(3), 846–852, DOI: [10.1021/acs.chemmater.2c03118](https://doi.org/10.1021/acs.chemmater.2c03118).
- 7 P. Shiri, V. Lai, T. Zepel, D. Griffin, J. Reifman, S. Clark, S. Grunert, L. P. E. Yunker, S. Steiner, H. Situ, *et al.*, Automated solubility screening platform using computer vision, *iScience*, 2021, 24(3), 102176, DOI: [10.1016/j.isci.2021.102176](https://doi.org/10.1016/j.isci.2021.102176).
- 8 B. Zhang, L. Merker, A. Sanin and H. S. Stein, Robotic cell assembly to accelerate battery research, *Digital Discovery*, 2022, 1, 755–762, DOI: [10.1039/d2dd00046f](https://doi.org/10.1039/d2dd00046f).
- 9 S. Li, E. R. Jira, N. H. Angello, J. Li, H. Yu, J. S. Moore, Y. Diao, M. D. Burke and C. M. Schroeder, Using automated synthesis to understand the role of side chains on molecular charge transport, *Nat. Commun.*, 2022, 13(1), 2102, DOI: [10.1038/s41467-022-29796-2](https://doi.org/10.1038/s41467-022-29796-2).
- 10 A. Narayanan Krishnamoorthy, C. Wölke, D. Diddens, M. Maiti, Y. Mabrouk, P. Yan, M. Grünebaum, M. Winter, A. Heuer and I. Cekic-Laskovic, Data-Driven Analysis of High-Throughput Experiments on Liquid Battery Electrolyte Formulations: Unraveling the Impact of Composition on Conductivity, *Chem.: Methods*, 2022, 2(9), e202200008, DOI: [10.1002/cmtd.202200008](https://doi.org/10.1002/cmtd.202200008).
- 11 S. Matsuda, K. Nishioka and S. Nakanishi, High-throughput combinatorial screening of multi-component electrolyte additives to improve the performance of Li metal secondary batteries, *Sci. Rep.*, 2019, 9(1), 6211, DOI: [10.1038/s41598-019-42766-x](https://doi.org/10.1038/s41598-019-42766-x).
- 12 L. Su, M. Ferrandon, J. A. Kowalski, J. T. Vaughey and F. R. Brushett, Electrolyte Development for Non-Aqueous Redox Flow Batteries Using a High-Throughput Screening Platform, *J. Electrochem. Soc.*, 2014, 161(12), A1905–A1914, DOI: [10.1149/2.0811412jes](https://doi.org/10.1149/2.0811412jes).
- 13 R. Duke, V. Bhat and C. Risko, Data storage architectures to accelerate chemical discovery: data accessibility for individual laboratories and the community, *Chem. Sci.*, 2022, 13(46), 13646–13656, DOI: [10.1039/d2sc05142g](https://doi.org/10.1039/d2sc05142g).
- 14 E. O. Pyzer-Knapp, C. Suh, R. Gómez-Bombarelli, J. Aguilera-Iparraguirre and A. Aspuru-Guzik, What Is High-Throughput Virtual Screening? A Perspective from Organic Materials Discovery, *Annu. Rev. Mater. Res.*, 2015, 45(1), 195–216, DOI: [10.1146/annurev-matsci-070214-020823](https://doi.org/10.1146/annurev-matsci-070214-020823).
- 15 R. Gómez-Bombarelli, J. Aguilera-Iparraguirre, T. D. Hirzel, D. Duvenaud, D. Maclaurin, M. A. Blood-Forsythe, H. S. Chae, M. Einzinger, D.-G. Ha, T. Wu, *et al.*, Design of efficient molecular organic light-emitting diodes by a high-throughput virtual screening and experimental approach, *Nat. Mater.*, 2016, 15(10), 1120–1127, DOI: [10.1038/nmat4717](https://doi.org/10.1038/nmat4717).
- 16 Q. Zhang, A. Khetan, E. Sorkun, F. Niu, A. Loss, I. Pucher and S. Er, Data-driven discovery of small electroactive molecules for energy storage in aqueous redox flow batteries, *Energy Storage Mater.*, 2022, 47, 167–177, DOI: [10.1016/j.ensm.2022.02.013](https://doi.org/10.1016/j.ensm.2022.02.013).
- 17 S. Matsuda, G. Lambard and K. Sodeyama, Data-driven automated robotic experiments accelerate discovery of multi-component electrolyte for rechargeable Li–O<sub>2</sub> batteries, *Cell Rep. Phys. Sci.*, 2022, 3(4), 100832, DOI: [10.1016/j.xcrp.2022.100832](https://doi.org/10.1016/j.xcrp.2022.100832).
- 18 M. Seifrid, R. Pollice, A. Aguilar-Granda, Z. Morgan Chan, K. Hotta, C. T. Ser, J. Vestfrid, T. C. Wu and A. Aspuru-Guzik, Autonomous Chemical Experiments: Challenges and Perspectives on Establishing a Self-Driving Lab, *Acc. Chem. Res.*, 2022, 55(17), 2454–2466, DOI: [10.1021/acs.accounts.2c00220](https://doi.org/10.1021/acs.accounts.2c00220).
- 19 B. P. Macleod, F. G. L. Parlane, C. C. Rupnow, K. E. Dettelbach, M. S. Elliott, T. D. Morrissey, T. H. Haley, O. Proskurin, M. B. Rooney, N. Taherimakhosousi, *et al.*, A self-driving laboratory advances the Pareto front for material properties, *Nat. Commun.*, 2022, 13(1), 995, DOI: [10.1038/s41467-022-28580-6](https://doi.org/10.1038/s41467-022-28580-6).
- 20 R. Pollice, G. Dos Passos Gomes, M. Aldeghi, R. J. Hickman, M. Krenn, C. Lavigne, M. Lindner-D'Addario, A. Nigam, C. T. Ser, Z. Yao, *et al.*, Data-Driven Strategies for Accelerated Materials Design, *Acc. Chem. Res.*, 2021, 54(4), 849–860, DOI: [10.1021/acs.accounts.0c00785](https://doi.org/10.1021/acs.accounts.0c00785).



- 21 A. Dave, J. Mitchell, K. Kandasamy, H. Wang, S. Burke, B. Paria, B. Póczos, J. Whitacre and V. Viswanathan, Autonomous Discovery of Battery Electrolytes with Robotic Experimentation and Machine Learning, *Cell Rep. Phys. Sci.*, 2020, **1**(12), 100264, DOI: [10.1016/j.xcrp.2020.100264](https://doi.org/10.1016/j.xcrp.2020.100264).
- 22 A. Dave, J. Mitchell, S. Burke, H. Lin, J. Whitacre and V. Viswanathan, Autonomous optimization of non-aqueous Li-ion battery electrolytes via robotic experimentation and machine learning coupling, *Nat. Commun.*, 2022, **13**(1), 5454, DOI: [10.1038/s41467-022-32938-1](https://doi.org/10.1038/s41467-022-32938-1).
- 23 A. Suzumura, H. Ohno, N. Kikkawa and K. Takechi, Finding a novel electrolyte solution of lithium-ion batteries using an autonomous search system based on ensemble optimization, *J. Power Sources*, 2022, **541**, 231698, DOI: [10.1016/j.jpowsour.2022.231698](https://doi.org/10.1016/j.jpowsour.2022.231698).
- 24 R. Shimizu, S. Kobayashi, Y. Watanabe, Y. Ando and T. Hitosugi, Autonomous materials synthesis by machine learning and robotics, *APL Mater.*, 2020, **8**(11), 111110, DOI: [10.1063/5.0020370](https://doi.org/10.1063/5.0020370).
- 25 N. Brandt, L. Griem, C. Herrmann, E. Schoof, G. Tosato, Y. Zhao, P. Zschumme and M. Selzer, Kadi4Mat: A Research Data Infrastructure for Materials Science, *Data Sci. J.*, 2021, **20**, 8, DOI: [10.5334/dsj-2021-008](https://doi.org/10.5334/dsj-2021-008).
- 26 C. Steinbeck, O. Koepler, F. Bach, S. Herres-Pawlis, N. Jung, J. Liermann, S. Neumann, M. Razum, C. Baldauf, F. Biedermann, *et al.*, NFDI4Chem - Towards a National Research Data Infrastructure for Chemistry in Germany, *Research Ideas and Outcomes*, 2020, **6**, e55852, DOI: [10.3897/rio.6.e55852](https://doi.org/10.3897/rio.6.e55852).
- 27 J. Potthoff, P. Tremouilhac, P. Hodapp, B. Neumair, S. Bräse and N. Jung, Procedures for systematic capture and management of analytical data in academia, *Anal. Chim. Acta: X*, 2019, **1**, 100007, DOI: [10.1016/j.acax.2019.100007](https://doi.org/10.1016/j.acax.2019.100007).
- 28 P. S. Gromski, J. M. Granda and L. Cronin, Universal Chemical Synthesis and Discovery with 'The Chemputer', *Trends Chem.*, 2020, **2**(1), 4–12, DOI: [10.1016/j.trechm.2019.07.004](https://doi.org/10.1016/j.trechm.2019.07.004).
- 29 A. J. S. Hammer, A. I. Leonov, N. L. Bell and L. Cronin, Chemputation and the Standardization of Chemical Informatics, *JACS Au*, 2021, **1**(10), 1572–1587, DOI: [10.1021/jacsau.1c00303](https://doi.org/10.1021/jacsau.1c00303).
- 30 Y. Jiang, H. Fakhruddin, G. Pizzuto, L. Longley, A. He, T. Dai, R. Clowes, N. Rankin and A. Cooper, Autonomous Biomimetic Solid Dispensing Using a Dual-Arm Robotic Manipulator, *Digital Discovery*, 2023, **2**, 1733–1744, DOI: [10.1039/d3dd00075c](https://doi.org/10.1039/d3dd00075c).
- 31 R. Tamura, K. Tsuda and S. Matsuda, NIMS-OS: an automation software to implement a closed loop between artificial intelligence and robotic experiments in materials science, *Sci. Technol. Adv. Mater.: Methods*, 2023, **3**(1), 2232297, DOI: [10.1080/27660400.2023.2232297](https://doi.org/10.1080/27660400.2023.2232297).
- 32 F. Rahmanian, J. Flowers, D. Guevarra, M. Richter, M. Fichtner, P. Donnelly, J. M. Gregoire and H. S. Stein, Enabling Modular Autonomous Feedback-Loops in Materials Science through Hierarchical Experimental Laboratory Automation and Orchestration, *Adv. Mater. Interfaces*, 2022, **9**(8), 2101987, DOI: [10.1002/admi.202101987](https://doi.org/10.1002/admi.202101987).
- 33 R. Hickman, M. Sim, S. Pablo-García, I. Woolhouse, H. Hao, Z. Bao, P. Bannigan, C. Allen, M. Aldeghi and A. Aspuru-Guzik, *Atlas: A Brain for Self-driving Laboratories*, American Chemical Society (ACS), 2023.
- 34 L. M. Roch, F. Häse, C. Kreisbeck, T. Tamayo-Mendoza, L. P. E. Yunker, J. E. Hein and A. Aspuru-Guzik, ChemOS: Orchestrating autonomous experimentation, *Sci. Robot.*, 2018, **3**(19), eaat5559, DOI: [10.1126/scirobotics.aat5559](https://doi.org/10.1126/scirobotics.aat5559).
- 35 J. F. Whitacre, J. Mitchell, A. Dave, W. Wu, S. Burke and V. Viswanathan, An Autonomous Electrochemical Test Stand for Machine Learning Informed Electrolyte Optimization, *J. Electrochem. Soc.*, 2019, **166**(16), A4181–A4187, DOI: [10.1149/2.0521916jes](https://doi.org/10.1149/2.0521916jes).
- 36 E. Fell and M. Aziz, *High-Throughput Electrochemical Characterization of Aqueous Organic Redox Flow Battery Active Material*, American Chemical Society (ACS), 2023.
- 37 I. Oh, M. A. Pence, N. G. Lukhanin, O. Rodríguez, C. M. Schroeder and J. Rodríguez-López, The Electrolab: An open-source, modular platform for automated characterization of redox-active electrolytes, *Device*, 1, 5, 100103, DOI: [10.1016/j.device.2023.100103](https://doi.org/10.1016/j.device.2023.100103).
- 38 M. N. Abd El-Hady, E. A. Gomaa and A. G. Al-Harazie, Cyclic voltammetry of bulk and nano CdCl<sub>2</sub> with ceftazidime drug and some DFT calculations, *J. Mol. Liq.*, 2019, **276**, 970–985, DOI: [10.1016/j.molliq.2018.10.125](https://doi.org/10.1016/j.molliq.2018.10.125).
- 39 B. Mekassa, M. Tessema, B. S. Chandravanshi, P. G. L. Baker and F. N. Muya, Sensitive electrochemical determination of epinephrine at poly(L-aspartic acid)/electro-chemically reduced graphene oxide modified electrode by square wave voltammetry in pharmaceuticals, *J. Electroanal. Chem.*, 2017, **807**, 145–153, DOI: [10.1016/j.jelechem.2017.11.045](https://doi.org/10.1016/j.jelechem.2017.11.045).
- 40 D. Nechaeva, A. Shishov, S. Ermakov and A. Bulatov, A paper-based analytical device for the determination of hydrogen sulfide in fuel oils based on headspace liquid-phase microextraction and cyclic voltammetry, *Talanta*, 2018, **183**, 290–296, DOI: [10.1016/j.talanta.2018.02.074](https://doi.org/10.1016/j.talanta.2018.02.074).
- 41 M. Li, S. A. Odom, A. R. Pancoast, L. A. Robertson, T. P. Vaid, G. Agarwal, H. A. Doan, Y. Wang, T. M. Suduwella, S. R. Bheemireddy, *et al.*, Experimental Protocols for Studying Organic Non-aqueous Redox Flow Batteries, *ACS Energy Lett.*, 2021, 3932–3943, DOI: [10.1021/acsenergylett.1c01675](https://doi.org/10.1021/acsenergylett.1c01675).
- 42 K. Wedege, D. Bae, W. A. Smith, A. Mendes and A. Bentien, Solar Redox Flow Batteries with Organic Redox Couples in Aqueous Electrolytes: A Minireview, *J. Phys. Chem. C*, 2018, **122**(45), 25729–25740, DOI: [10.1021/acs.jpcc.8b04914](https://doi.org/10.1021/acs.jpcc.8b04914).
- 43 P. Jittiarporn, S. Lek, K. Kooptarnond, W. Taweepreda, P. Chooto and M. Khangkhamano, Synthesis of h-MoO<sub>3</sub> and (NH<sub>4</sub>)<sub>2</sub>Mo<sub>4</sub>O<sub>13</sub> Using Precipitation Method at Various pH Values and their Photochromic Properties, *Appl. Mech. Mater.*, 2016, **835**, 34–41, DOI: [10.4028/www.scientific.net/AMM.835.34](https://doi.org/10.4028/www.scientific.net/AMM.835.34).
- 44 S. Rakhshan Pouri, M. Manic and S. Phongikaroon, A novel framework for intelligent signal detection via artificial neural networks for cyclic voltammetry in pyroprocessing





- technology, *Ann. Nucl. Energy*, 2018, **111**, 242–254, DOI: [10.1016/j.anucene.2017.09.002](https://doi.org/10.1016/j.anucene.2017.09.002).
- 45 J. Massah and K. Asefpour Vakilian, An intelligent portable biosensor for fast and accurate nitrate determination using cyclic voltammetry, *Biosyst. Eng.*, 2019, **177**, 49–58, DOI: [10.1016/j.biosystemseng.2018.09.007](https://doi.org/10.1016/j.biosystemseng.2018.09.007).
- 46 Django Software Foundation, *Django 2.2*, 2019, <https://djangoproject.com>.
- 47 MongoDB, <https://www.mongodb.com/>.
- 48 Apache License Version 2.0, January 2004, <https://www.apache.org/>.
- 49 KINOVA KORTEX API, <https://github.com/Kinovarobotics/kortex/>.
- 50 A. Jain, S. P. Ong, W. Chen, B. Medasani, X. Qu, M. Kocher, M. Brafman, G. Petretto, G. M. Rignanese, G. Hautier, *et al.*, FireWorks: a dynamic workflow system designed for high-throughput applications, *Concurrency Comput. Pract. Ex.*, 2015, **27**(17), 5037–5059, DOI: [10.1002/cpe.3505](https://doi.org/10.1002/cpe.3505).
- 51 Tkinter, <https://tkdocs.com/>.
- 52 Kinova, <https://www.kinovarobotics.com/>.
- 53 Pine Research, <https://pineresearch.com/>.
- 54 ExpFlow, <https://d3tales.as.uky.edu/expflow/>.
- 55 F. Pezoa, J. L. Reutter, F. Suarez, M. Ugarte and D. Vrgo, *Foundations of JSON Schema*, 2016.
- 56 R. Duke, V. Bhat, P. Sornberger, S. A. Odom and C. Risko, Towards a comprehensive data infrastructure for redox-active organic molecules targeting non-aqueous redox flow batteries, *Digital Discovery*, 2023, **2**, 1152–1162, DOI: [10.1039/d3dd00081h](https://doi.org/10.1039/d3dd00081h).
- 57 N. Elgrishi, K. J. Rountree, B. D. Mccarthy, E. S. Rountree, T. T. Eisenhart and J. L. Dempsey, A Practical Beginner's Guide to Cyclic Voltammetry, *J. Chem. Educ.*, 2018, **95**(2), 197–206, DOI: [10.1021/acs.jchemed.7b00361](https://doi.org/10.1021/acs.jchemed.7b00361).
- 58 L. M. Moshurchak, W. M. Lamanna, M. Bulinski, R. L. Wang, R. R. Garsuch, J. Jiang, D. Magnuson, M. Triemert and J. R. Dahn, High-Potential Redox Shuttle for Use in Lithium-Ion Batteries, *J. Electrochem. Soc.*, 2009, **156**(4), A309, DOI: [10.1149/1.3077578](https://doi.org/10.1149/1.3077578).
- 59 Y. Huo, X. Xing, C. Zhang, X. Wang and Y. Li, An all organic redox flow battery with high cell voltage, *RSC Adv.*, 2019, **9**(23), 13128–13132, DOI: [10.1039/c9ra01514k](https://doi.org/10.1039/c9ra01514k).
- 60 L. Zhang, Z. Zhang, P. C. Redfern, L. A. Curtiss and K. Amine, Molecular engineering towards safer lithium-ion batteries: a highly stable and compatible redox shuttle for overcharge protection, *Energy Environ. Sci.*, 2012, **5**(8), 8204–8207, DOI: [10.1039/C2EE21977H](https://doi.org/10.1039/C2EE21977H).
- 61 S. I. Etkind, J. Lopez, Y. G. Zhu, J.-H. Fang, W. J. Ong, Y. Shao-Horn and T. M. Swager, Thianthrene-Based Bipolar Redox-Active Molecules Toward Symmetric All-Organic Batteries, *ACS Sustain. Chem. Eng.*, 2022, **10**(36), 11739–11750, DOI: [10.1021/acssuschemeng.2c01717](https://doi.org/10.1021/acssuschemeng.2c01717).
- 62 S. Ergun, C. F. Elliott, A. P. Kaur, S. R. Parkin and S. A. Odom, Controlling Oxidation Potentials in Redox Shuttle Candidates for Lithium-Ion Batteries, *J. Phys. Chem. C*, 2014, **118**(27), 14824–14832, DOI: [10.1021/jp503767h](https://doi.org/10.1021/jp503767h).
- 63 G. Kwon, K. Lee, M. H. Lee, B. Lee, S. Lee, S.-K. Jung, K. Ku, J. Kim, S. Y. Park, J. E. Kwon, *et al.*, Bio-inspired Molecular Redesign of a Multi-redox Catholyte for High-Energy Non-aqueous Organic Redox Flow Batteries, *Chem*, 2019, **5**(10), 2642–2656, DOI: [10.1016/j.chempr.2019.07.006](https://doi.org/10.1016/j.chempr.2019.07.006).
- 64 Z. Liang, N. H. Attanayake, K. V. Greco, B. J. Neyhouse, J. L. Barton, A. P. Kaur, W. L. Eubanks, F. R. Brushett, J. Landon and S. A. Odom, Comparison of Separators vs Membranes in Nonaqueous Redox Flow Battery Electrolytes Containing Small Molecule Active Materials, *ACS Appl. Energy Mater.*, 2021, **4**(6), 5443–5451, DOI: [10.1021/acsaem.1c00017](https://doi.org/10.1021/acsaem.1c00017).
- 65 A. J. Prins, A. Dumitrascu, N. J. Mortimer, D. R. Henton and T. F. Guarr, High Potential Organic Materials for Battery Applications, *ECS Trans.*, 2017, **80**(10), 97, DOI: [10.1149/08010.0097ecst](https://doi.org/10.1149/08010.0097ecst).
- 66 Y. Wang, E. I. Rogers and R. G. Compton, The measurement of the diffusion coefficients of ferrocene and ferrocenium and their temperature dependence in acetonitrile using double potential step microdisk electrode chronoamperometry, *J. Electroanal. Chem.*, 2010, **648**(1), 15–19, DOI: [10.1016/j.jelechem.2010.07.006](https://doi.org/10.1016/j.jelechem.2010.07.006).
- 67 C. G. Armstrong, R. W. Hogue and K. E. Toghiani, Characterisation of the ferrocene/ferrocenium ion redox couple as a model chemistry for non-aqueous redox flow battery research, *J. Electroanal. Chem.*, 2020, **872**, 114241, DOI: [10.1016/j.jelechem.2020.114241](https://doi.org/10.1016/j.jelechem.2020.114241).
- 68 M. Li, Z. Rhodes, J. R. Cabrera-Pardo and S. D. Minter, Recent advancements in rational design of non-aqueous organic redox flow batteries, *Sustainable Energy Fuels*, 2020, **4**(9), 4370–4389, DOI: [10.1039/d0se00800a](https://doi.org/10.1039/d0se00800a).
- 69 J. D. Milshtein, A. P. Kaur, M. D. Casselman, J. A. Kowalski, S. Modekrutti, P. L. Zhang, N. Harsha Attanayake, C. F. Elliott, S. R. Parkin, C. Risko, *et al.*, High current density, long duration cycling of soluble organic active species for non-aqueous redox flow batteries, *Energy Environ. Sci.*, 2016, **9**(11), 3531–3543, DOI: [10.1039/c6ee02027e](https://doi.org/10.1039/c6ee02027e).
- 70 A. S. Perera, T. M. Suduwella, N. H. Attanayake, R. K. Jha, W. L. Eubanks, I. A. Shkrob, C. Risko, A. P. Kaur and S. A. Odom, Large variability and complexity of isothermal solubility for a series of redox-active phenothiazines, *Mater. Adv.*, 2022, **3**(23), 8705–8715, DOI: [10.1039/d2ma00598k](https://doi.org/10.1039/d2ma00598k).
- 71 B. G. Tegegne, D. M. Kabtamu, Y.-Z. Li, Y.-T. Ou, Z.-J. Huang, N.-Y. Hsu, H.-H. Ku, Y.-M. Wang and C.-H. Wang, N-methylphenothiazine as stable and low-cost catholyte for nonaqueous organic redox flow battery, *J. Energy Storage*, 2023, **61**, 106753, DOI: [10.1016/j.est.2023.106753](https://doi.org/10.1016/j.est.2023.106753).
- 72 G. Kwon, S. Lee, J. Hwang, H.-S. Shim, B. Lee, M. H. Lee, Y. Ko, S.-K. Jung, K. Ku, J. Hong, *et al.*, Multi-redox Molecule for High-Energy Redox Flow Batteries, *Joule*, 2018, **2**(9), 1771–1782, DOI: [10.1016/j.joule.2018.05.014](https://doi.org/10.1016/j.joule.2018.05.014).
- 73 K. Nihon, Electron-Transfer Kinetics of Nitroxide Radicals as an Electrode-Active Material, *Bull. Chem. Soc. Jpn.*, 2004, **77**(12), 2203–2204, DOI: [10.1246/bcsj.77.2203](https://doi.org/10.1246/bcsj.77.2203).
- 74 P. J. Peerce and A. J. Bard, Polymer films on electrodes: Part II. Film structure and mechanism of electron transfer with electrodeposited poly(vinylferrocene), *J. Electroanal. Chem.*



- Interfacial Electrochem.*, 1980, **112**(1), 97–115, DOI: [10.1016/S0022-0728\(80\)80011-8](https://doi.org/10.1016/S0022-0728(80)80011-8).
- 75 G. D. De La Garza, A. P. Kaur, I. A. Shkrob, L. A. Robertson, S. A. Odom and A. J. Mcneil, Soluble and stable symmetric tetrazines as anolytes in redox flow batteries, *J. Mater. Chem. A*, 2022, **10**(36), 18745–18752, DOI: [10.1039/d2ta04515j](https://doi.org/10.1039/d2ta04515j).
- 76 J. Kim, H. Kim, S. Lee, G. Kwon, T. Kang, H. Park, O. Tamwattana, Y. Ko, D. Lee and K. Kang, A p–n fusion strategy to design bipolar organic materials for high-energy-density symmetric batteries, *J. Mater. Chem. A*, 2021, **9**(25), 14485–14494, DOI: [10.1039/d1ta02059e](https://doi.org/10.1039/d1ta02059e).
- 77 M. E. Speer, M. Kolek, J. J. Jassoy, J. Heine, M. Winter, P. M. Bieker and B. Esser, Thianthrene-functionalized polynorbornenes as high-voltage materials for organic cathode-based dual-ion batteries, *Chem. Commun.*, 2015, **51**(83), 15261–15264, DOI: [10.1039/c5cc04932f](https://doi.org/10.1039/c5cc04932f).
- 78 Z. Li, S. Li, S. Liu, K. Huang, D. Fang, F. Wang and S. Peng, Electrochemical Properties of an All-Organic Redox Flow Battery Using 2,2,6,6-Tetramethyl-1-Piperidinyloxy and N-Methylphthalimide, *Electrochem. Solid-State Lett.*, 2011, **14**(12), A171, DOI: [10.1149/2.012112esl](https://doi.org/10.1149/2.012112esl).
- 79 S. Minteer, J. Chen, S. Lin, C. Crudden, S. Dehnen, P. V. Kamat, M. Kozlowski, G. Masson and S. J. Miller, New Guidelines for Presenting Electrochemical Data in All ACS Journals, *ACS Catal.*, 2023, **13**(7), 4468–4469, DOI: [10.1021/acscatal.3c00995](https://doi.org/10.1021/acscatal.3c00995).
- 80 B. Cao, L. A. Adutwum, A. O. Oliynyk, E. J. Luber, B. C. Olsen, A. Mar and J. M. Buriak, How To Optimize Materials and Devices via Design of Experiments and Machine Learning: Demonstration Using Organic Photovoltaics, *ACS Nano*, 2018, **12**(8), 7434–7444, DOI: [10.1021/acsnano.8b04726](https://doi.org/10.1021/acsnano.8b04726).

